Cancer cell angiogenic capability is regulated by 3D culture and integrin engagement

Claudia Fischbach[a,b], Hyun Joon Kong[a,c], Susan X. Hsiong[a], Marta B. Evangelista[a,d,e], Will Yuen[a], and David J. Mooney[a,f,1]

[a]School of Engineering and Applied Sciences, Harvard University, 40 Oxford Street, Cambridge, MA 02138; [b]Department of Biomedical Engineering, Cornell University, 157 Weill Hall, Ithaca, NY 14853; [c]Department of Chemical and Biomolecular Engineering, University of Illinois at Urbana–Champaign, Urbana, IL 61801; [d]Instituto de Engenharia Biomedica, Divisao de Biomateriais, Rua do Campo Alegre, 823, 4150-180 Porto, Portugal; [e]Universidade do Porto, Faculdade de Engenharia, Departamento de Engenharia Metalúrgica e de Materiais, Rua Dr. Roberto Frias s/n, 4200-465 Porto, Portugal; and [f]Wyss Institute of Biologically Inspired Engineering, Harvard University, Cambridge, MA 02138

Edited by Robert Langer, Massachusetts Institute of Technology, Cambridge, MA, and approved November 26, 2008 (received for review September 9, 2008)

Three-dimensional culture alters cancer cell signaling; however, the underlying mechanisms and importance of these changes on tumor vascularization remain unclear. A hydrogel system was used to examine the role of the transition from 2D to 3D culture, with and without integrin engagement, on cancer cell angiogenic capability. Three-dimensional culture recreated tumor microenvironmental cues and led to enhanced interleukin 8 (IL-8) secretion that depended on integrin engagement with adhesion peptides coupled to the polymer. In contrast, vascular endothelial growth factor (VEGF) secretion was unaffected by 3D culture with or without substrate adhesion. IL-8 diffused greater distances and was present in higher concentrations in the systemic circulation, relative to VEGF. Implantation of a polymeric IL-8 delivery system into GFP bone marrow-transplanted mice revealed that localized IL-8 up-regulation was critical to both the local and systemic control of tumor vascularization in vivo. In summary, 3D integrin engagement within tumor microenvironments regulates cancer cell angiogenic signaling, and controlled local and systemic blockade of both IL-8 and VEGF signaling may improve antiangiogenic therapies.

ECM | microenvironment | tumor vascularization | drug delivery | IL-8

Changes of the microenvironment are fundamental to tumorigenesis, and 3D cultures may be used to study the mechanisms and effects by which these alterations modulate cancer cell signaling (1). Pathologically relevant cancer models have been developed by culturing tumor cells within natural and synthetic extracellular matrix (ECM) mimics, and 3D microenvironmental conditions within these culture systems clearly alter tumor cell signaling (2, 3). However, the multiple variables typically inherent in the transition from 2D to 3D make it difficult to define the underlying mechanisms and importance of these changes. For example, there may simultaneously exist differences in the soluble environment because of substances diffusing through or from the adhesion substrate, central hypoxia, and polarity of cell adhesion. Comparison between tumor cells seeded onto ECM-coated 2D culture dishes and encapsulated within 3D ECM gels can be further complicated by differing mechanical properties of the adhesion substrate in each situation that can alter tumor cell behavior (4).

Tumor vascularization represents a hallmark of cancer, and we have developed an artificial ECM culture system to examine the role of the transition from 2D to 3D culture on tumor vascularization, in the absence or presence of integrin engagement under constant chemical and physical properties. Tumor vascularization is mediated by an overbalance of proangiogenic molecules that may be caused by dysregulated cell–ECM interactions (5). Vascular endothelial growth factor (VEGF), basic fibroblast growth factor (bFGF), and IL-8, in particular, have been widely investigated for their role in tumor vascularization, and their signaling is regulated by both cell–ECM interactions and 3D culture conditions (3, 6, 7). Because integrin engagement with ECM molecules is differentially regulated in 2D relative to 3D culture (3, 8), it is likely that these changes underlie the tumor angiogenic switch. We provide experimental evidence that the integrated effects of 3D tumor microenvironmental cues and 3D integrin engagement differentially regulate VEGF and IL-8 secretion and that these differences impact tumor vascularization in vivo. These findings serve to identify 3D integrin engagement as a mechanism that alters cancer cell angiogenic signaling and that may be explored toward more efficacious antiangiogenic therapies.

Results and Discussion

The roles of 3D culture and integrin engagement on cancer cell angiogenic potential were examined with oral squamous cell carcinoma cells (OSCC-3) and a synthetic ECM of alginate hydrogels containing covalently coupled RGD adhesion peptides at a density that correlates to the number of RGD adhesion sites in tumors in vivo (9). OSCC-3 cells were chosen because they are representative of a particularly aggressive epithelial malignancy that is mediated in large part by its microenvironmentally controlled angiogenic potential (10). Alginates gel in the presence of divalent cations (e.g., Ca^{2+}), yielding matrices with controlled mechanical properties ($\approx$60 kDa in our studies) and pore sizes that degrade very slowly and by a mechanism that is independent of cell-secreted proteolytic enzymes (11). Consequently, alginate hydrogels provide controllable and constant chemical and physical conditions to adherent or encapsulated cells, as contrasted with many other natural biopolymers (e.g., Matrigel, collagen).

Alginates are typically nonadhesive to cells, but chemical modification with RGD, the primary integrin recognition site contained in many ECM proteins (e.g., fibronectin) (12), readily allowed OSCC-3 to adhere onto topographically flat films of these gels (Fig. 1*A*). To develop a pathologically relevant mimic of the ECM found in tumors in vivo, alginates were modified with RGD peptides to yield matrices that recreated the density of RGD adhesion sites of tumor-associated ECM in vivo (RGD-alginates, 8.0×10^{16} per mL matrix; tumor-associated ECM, 8.6×10^{16} per mL matrix). OSCC-3 attached onto RGD-alginate surfaces in a quantitatively similar but less spread manner compared with tissue culture plastic (TCPS) and fibronectin-coated TCPS (Fig. 1*A*). Inhibition of $\alpha5\beta1$ and $\alpha v\beta3$ integrins (i.e., the two predominant receptors involved in binding ECM molecules with RGD domains) by specific antibodies indicated that cells predominantly engage $\alpha5\beta1$ integrins to interact with RGD-modified alginate substrates because decreased OSCC-3 adhesion and proliferation were observed in response to anti-$\alpha5\beta1$ treatment, but not blockade of $\alpha v\beta3$ (Fig. 1*B*). Additionally, OSCC-3 cultured on these matrices secreted the proangiogenic factors VEGF, IL-8, and bFGF in a manner comparable with other

Author contributions: C.F. and D.J.M. designed research; C.F., H.J.K., S.X.H., M.B.E., and W.Y. performed research; H.J.K., S.X.H., and W.Y. contributed new reagents/analytic tools; C.F., H.J.K., and D.J.M. analyzed data; and C.F. and D.J.M. wrote the paper.

The authors declare no conflict of interest.

This article is a PNAS Direct Submission.

[1]To whom correspondence should be addressed. E-mail: mooneyd@seas.harvard.edu.

This article contains supporting information online at www.pnas.org/cgi/content/full/0808932106/DCSupplemental.

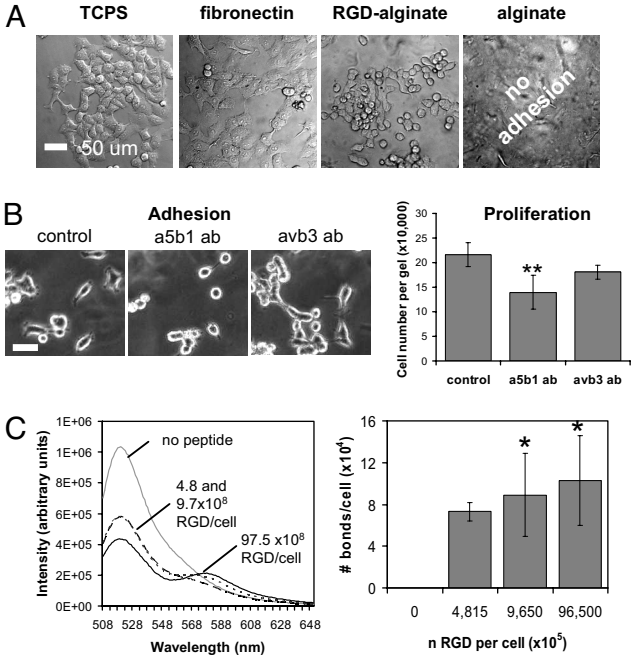

Fig. 1. Cell binding and integrin engagement. (*A*) Two-dimensional adhesion studies verified that OSCC-3 adhered to RGD-functionalized alginate in a manner comparable with TCPS and TCPS coated with fibronectin (fibronectin), whereas seeding cells on nonmodified alginate matrices (alginate) did not result in cell adhesion. (*B*) Inhibition of $\alpha5\beta1$ integrins with function blocking antibodies (a5b1 ab) decreased adhesion and proliferation of OSCC-3 on 2D RGD-alginate substrates compared with control conditions, whereas no statistically significant differences were detected after inhibition of $\alpha v\beta3$ integrins (avb3 ab). (Scale bar: 50 μm.) **, $P < 0.01$. (*C*) FRET analysis to quantify the number of receptor–ligand bonds formed between cells in 3D culture and RGD peptides coupled to the polymer. Increasing the number of RGD peptides significantly increased integrin engagement by RGD-functionalized alginates as detected by increased energy transfer (decreased donor fluorescein emission intensity at $\lambda = 520$ nm; increased acceptor emission at $\lambda = 580$ nm). *, $P < 0.05$. Changes in energy transfer were translated into absolute bond numbers per cell as a function of the number of RGD ligands available to each cell (n RGD per cell), as described in ref. 7, and no bonds were noted in the absence of RGD ligands.

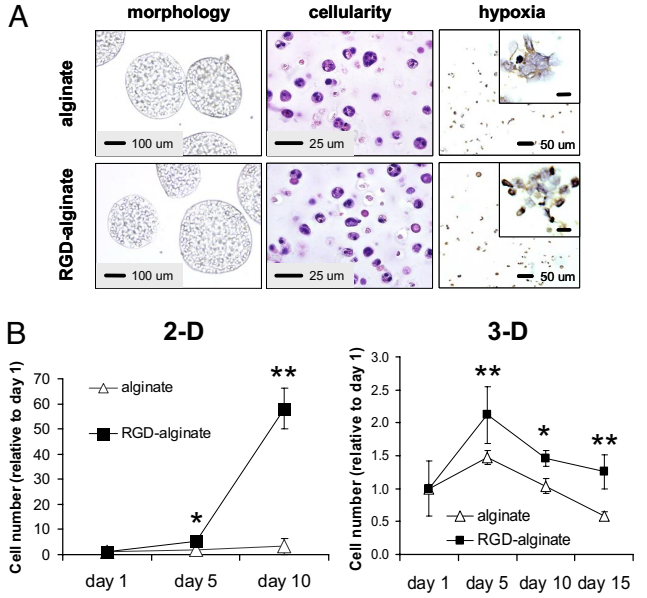

Fig. 2. Histological characteristics and cell proliferation in 2D and 3D alginate cultures. (*A*) Images of cells cultured within gels prepared from unmodified (alginate) or RGD-modified alginate (RGD-alginate) displayed qualitatively similar morphologies and cellularity as detected by microscopic evaluation of tumor spheroids and H&E-stained histological cross-sections, respectively. Hypoxia, as determined by immunohistological staining for the hypoxia marker Hypoxyprobe (brown stain; most visible in magnified *Insets*) developed in both culture systems. (*Inset* scale bars: 10 μm.) (*B*) Integrin engagement allowed for tumor cell proliferation when cells were cultured on (2D) or in (3D) RGD-modified alginate gels, whereas no proliferation occurred in the absence of cell–matrix interactions (alginate) in either 2D or 3D culture. Cellularity at later stages of 3D culture was controlled by integrin engagement. *, $P < 0.05$; **, $P < 0.01$.

commonly used 2D culture substrates [supporting information (SI) Fig. S1; bFGF was secreted at negligible levels on all surfaces; data not shown]. The differences in IL-8 secretion on RGD-modified alginate, TCPS, and fibronectin-coated TCPS in 2D culture were statistically significant; however, these changes were minor compared with the markedly greater differences in secretion with 3D culture noted below.

Adhesion ligand–receptor bond formation was next analyzed with a recently developed FRET technique (13) to confirm the ability of this system specifically to modulate integrin engagement in 3D culture. Enhancing the number of RGD peptides in the gels increased the extent of energy transfer between the fluorescent tags on the ligands and the cells (Fig. 1*C*), and calculation of bond numbers from these data confirmed that the number of cell bonds to RGD-coupled alginate significantly increased with RGD density (Fig. 1*C*). Analysis of $\alpha5\beta1$ integrin subunit expression by flow cytometry verified that the polymer itself did not affect integrin expression because cells cultured on 2D RGD-alginate disks expressed similar levels of $\alpha5\beta1$ relative to conventional monolayer culture (Fig. S2*A*). Three-dimensional culture within RGD-alginate slightly modulated $\alpha5\beta1$ expression (Fig. S2*A*), but integrin expression levels were similar in 3D for matrices that either promoted (RGD-alginate) or did not mediate integrin engagement [unmodified alginate, or alginate modified with a nonsense (RGE) peptide] (Fig. S2*B*), suggesting that transition from 2D to 3D, but not the cell material interactions per se have an effect on integrin expression. Altogether, these data validate the relevance of this culture system to study tumor cells in 3D culture in the absence or presence of a specific mechanism of adhesion.

Microenvironmental conditions critical to the growth and angiogenic capacity of tumor cells were recreated by 3D alginate culture, and both the transition to 3D culture and integrin engagement impacted cell proliferation and survival. In both unmodified and RGD-modified alginate, tumor cells were distributed evenly throughout the matrix, had cell–cell interactions upon proliferation, and were exposed to hypoxia (Fig. 2*A*), a key regulatory factor of VEGF, bFGF, and IL-8 (14, 15). Cell–ECM interactions may control the growth rate of tumor cells in 3D culture (16), and in this system integrin engagement also promoted proliferation of OSCC-3 in both 2D and 3D cultures (Fig. 2*B*). Analysis of cell viability, furthermore, indicated that integrin engagement promoted long-term cell viability (Fig. S3*A*), and this may relate to integrin signaling that allows tumor cells to adapt to adverse conditions (e.g., limited oxygen and nutrient supply) at later time points of 3D culture or in tumor formation in vivo (17). Proliferation of 3D cultured U87 glioblastoma and MDA-MB231 breast cancer cells was similarly enhanced within RGD-modified alginate matrices relative to culture within unmodified substrates, indicating that the results described above are not unique to OSCC-3 cells, but may be broadly applicable to other cancer cells (Fig. S3*B*).

VEGF, bFGF, and IL-8 secretion were quantified to investigate the effect of tumor microenvironmental conditions and integrin engagement on the angiogenic phenotype of tumor cells. Transition from 2D culture to 3D culture in the absence of cell adhesion ligands in the gels led to a 17-fold increase in IL-8 secretion at day 5 of culture, whereas IL-8 secretion was increased 35-fold during this transition when cell adhesion ligands were present in the gels

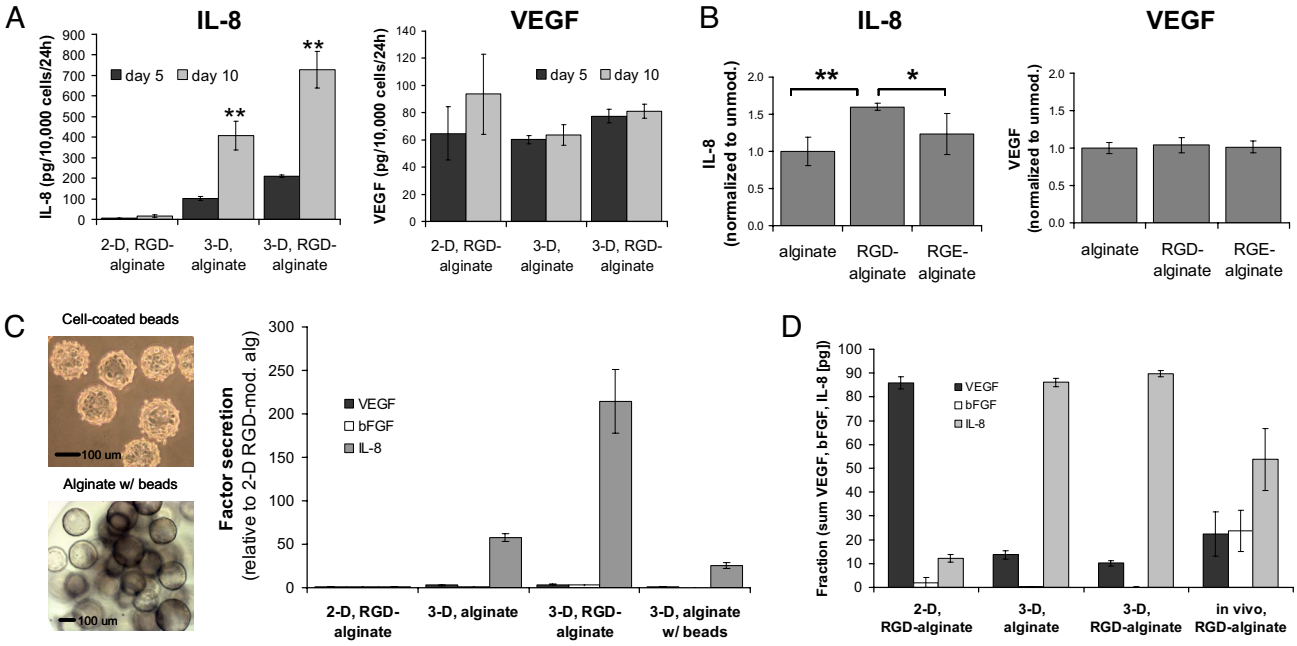

Fig. 3. Angiogenic characteristics of tumor cells cultured in 2D and 3D alginate systems. (*A*) Three-dimensional culture (3D, RGD-alginate) resulted in dramatically enhanced IL-8 levels relative to 2D culture (2D, RGD-alginate), and integrin engagement was critical to this end as determined by ELISA of conditioned medium from 3D cultures within unmodified (3D, alginate) and RGD-modified alginate (3D, RGD-alginate). No significant differences were detected between VEGF secretion in 2D (2D, RGD-alginate) and 3D cell culture (3D, RGD-alginate), and 3D integrin engagement increased VEGF secretion in 3D cultures only slightly. (*B*) Three-dimensional control experiments with nonadhesive RGE-alginate resulted in diminished secretion of IL-8 (*, $P < 0.05$; **, $P < 0.01$), whereas VEGF secretion was similar for cultures within nonadhesive (alginate, RGE-alginate) and adhesive (RGD-alginate) matrices. (*C*) Analysis of the contribution of the 3D environment and 3D integrin engagement. Cytodex beads were coated in a 2D manner with OSCC-3 (cell-coated beads) and subsequently encapsulated within 3D alginate (alginate, w/beads). IL-8 secretion for this condition was enhanced relative to 2D cultures (2D, RGD-alginate) but was lower compared with both 3D conditions (3D, alginate and 3D, RGD-alginate). No remarkable differences were detected for VEGF and bFGF secretion under these conditions. (*D*) VEGF, bFGF, and IL-8 secretion presented as a fraction of the total secretion of angiogenic factors (in picograms per 10,000 cells). The effects of 3D microenvironmental conditions and 3D integrin engagement were determined by comparing 2D cultures on RGD alginate, 3D culture within alginate and RGD-alginate, and tumors formed in vivo. Data bars are small where not visible.

(Fig. 3*A*); an even more dramatic up-regulation of IL-8 secretion with 3D culture was noted at day 10 (i.e., 46-fold for transition from 2D RGD-alginate to 3D RGD-alginate) (Fig. 3*A*). In contrast, VEGF secretion was only modestly modulated by these conditions (Fig. 3*A*), and negligible bFGF secretion was detected independently of culture conditions and integrin engagement (data not shown). Measurement of total factor secretion as a sum of both factor released into the culture medium and factor sequestered within the synthetic ECMs verified that these differences were related to changes in angiogenic factor secretion rather than altered factor deposition within the 2D and 3D culture matrices (Fig. S4*A*). Approximately 25% of secreted VEGF was retained throughout all experimental conditions, whereas ≈93% of secreted bFGF remained associated with the different alginate substrates (Fig. S4*B*). Although bFGF was deposited at a much higher rate within the materials, the overall amount of released bFGF was still very low compared with the other investigated factors. IL-8 deposition was remarkably greater in the 2D relative to 3D matrices, but this effect was likely attributable to the low secretion in this condition rather than saturation of the factor inside the gel (Fig. S4*C*). Comparison of factor secretion from OSCC-3 within gels containing no adhesion ligands, RGD ligands, or a control peptide not mediating integrin engagement (RGE) further confirmed the independence of VEGF and bFGF secretion and the dependence of IL-8 secretion on integrin engagement (Fig. 3*B*; bFGF not shown). These control experiments verified that the observed increase in IL-8 secretion is specific to cellular interactions with RGD peptides and not because of differential adsorption or retention of endogenous proteins (e.g., fibronectin) with changes in the alginate chemistry.

The dramatic up-regulation of IL-8 expression may be broadly applicable to other tumor cell types because 3D culture with different matrices and tumor cell lines similarly resulted in significant up-regulation of IL-8 (3, 18). Examination of IL-8 release by U87 glioblastoma cells confirmed that both 3D microenvironmental conditions and integrin engagement are critical to IL-8 secretion by these cells (Fig. S5). Similarly, MDA-MB231 breast cancer cells up-regulated IL-8 secretion in response to 3D integrin engagement but, interestingly, not in response to transition from 2D to 3D culture (Fig. S5). These results underline the angiogenic heterogeneity of different types of cancer and are particularly remarkable because elevated IL-8 expression by MDA-MB231 cells seems to be an indicator of enhanced metastatic potential of these cells relative to MCF-7 breast cancer cells, which were shown to exhibit increased IL-8 secretion in 3D vs. 2D culture (3, 19). Consequently, alginate-based artificial ECMs may provide novel tools that may help to identify the severity of an individual's cancer based on the ability of the tumor cell to respond to 3D culture conditions and integrin engagement.

Previous studies suggest that enhanced IL-8 expression may be related to changes in cell morphology as alterations of the actin cytoskeleton lead to differential activation of NFκB, a transcription factor that induces IL-8 expression (20). Because of these connections between IL-8 expression, integrin engagement, and cell morphology, we hypothesized that IL-8 up-regulation within 3D RGD-modified cultures may be attributed to the integrated effects of integrin engagement and changes in cell morphology relative to 2D cultures. To address this hypothesis and to elucidate more fully the contribution of the 3D environment, experiments were performed in which integrins were engaged in a 2D manner with beads that were subsequently embedded in nonmodified alginate gels (Fig. 3*C* and Fig. S6). This procedure resulted in 3D spheres that were similar in size to 3D cultures prepared from either nonmodified or RGD-modified alginate (Fig. 3*C*; Fig. S6). Interestingly, IL-8

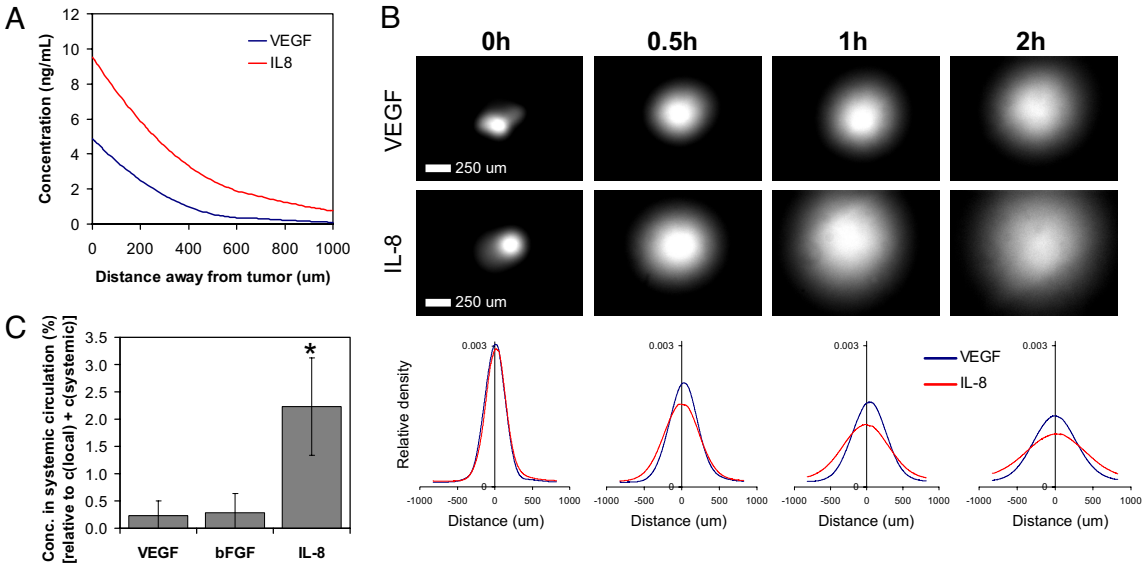

Fig. 4. Analysis of local and systemic proangiogenic signaling. (*A*) Mathematical modeling of VEGF and IL-8 concentrations in the tissue surrounding the tumor as a result of diffusion, elimination, and secretion predicts that IL-8 will be present at greater concentrations, compared with VEGF, and is more likely to reach the systemic circulation. (*B*) IL-8 is more broadly distributed throughout the surrounding pseudotissue (Matrigel) than VEGF in vitro. Specifically, IL-8 diffuses away from an initial point source (0 h) more readily, relative to VEGF, as determined by diffusion analysis of fluorescently labeled VEGF and IL-8 within Matrigel after 0.5 h, 1 h, and 2 h. Spatial distribution curves generated by densitometric image analysis show average values ($n = 4$). (*C*) Calculation of the normalized systemic concentrations of angiogenic factors (fraction of the sum of the concentration in the local tumor microenvironment and the systemic circulation as calculated based on the total volume of each tumor and a mouse blood volume of ≈72 mL/kg) confirmed that IL-8 is available in the systemic circulation to a much greater extent than the other two factors. *, $P < 0.05$.

secretion in 3D bead cultures was significantly enhanced compared with 2D RGD alginate cultures, but it was lower relative to 3D culture within either nonmodified or RGD-modified matrices (Fig. 3*C*). These results suggest that the 3D environment clearly plays an important role in the regulation of IL-8 secretion but that the integrated effects of 3D environment, 3D cell morphology, and 3D integrin engagement are necessary to stimulate IL-8 release by tumor cells fully. Typical characteristics of 3D tumor microenvironments (both in vitro and in vivo) have been associated with increased IL-8 secretion. In particular, hypoxia, limited nutrient supply, and low pH caused by restricted removal of metabolic products lead to up-regulation of IL-8 (21); however, until now it remained unclear to what extent the effect of these conditions is modulated by 3D cell–ECM interactions. For example, hypoxia is commonly considered an important regulator of IL-8 expression, but our results together with our published data using 2D cultures under reduced oxygen tension (3) indicate that its sole contribution is comparably small and that the combined effects of hypoxia and 3D integrin engagement may be necessary to elicit IL-8-mediated tumorigenic responses fully.

Reciprocal interactions among VEGF, bFGF, and IL-8 may be critical to tumor angiogenesis (22, 23), and analysis of the relative contribution of these factors as a percentage of their cumulative secretion into culture medium revealed that VEGF was the major secreted angiogenic factor in 2D culture on RGD-alginate (86% of total; Fig. 3*D*). In marked contrast, IL-8 secretion was the major secreted angiogenic factor (90% of total) in 3D culture. Interestingly, lysates prepared from OSCC-3 tumors grown within RGD-alginate in vivo contained VEGF and IL-8 at concentrations comparable with 3D culture (Fig. 3*D*), an increased bFGF contribution not noted in 3D in vitro culture that may be related to inflammatory cell signaling (24). Similar results were obtained when secretion values were evaluated in terms of the molarity of the individual growth factors (data not shown) and when total factor secretion (i.e., both factors secreted into the culture medium and sequestered within the 2D and 3D alginate matrices) in vitro was compared with in vivo lysate content (Fig. S7). These findings indicate that IL-8 may play a more prominent role in tumor angiogenesis than typically assumed and were consistent with our previous results using poly(lactide-coglycolide) (PLG)-based polymeric scaffolds that do not allow for specific control over 3D integrin engagement (3). In summary, 3D culture systems using synthetic ECMs may be useful in identifying molecular mechanisms involved in the differential regulation of VEGF and IL-8 signaling. However, coculture approaches [e.g., with inflammatory cells (24)] may be necessary to recreate certain paracrine signaling conditions that may be implicated in regulating bFGF secretion in vivo. Because of the relatively insignificant role of bFGF in the previous experiments, the next series of studies focused on the role of VEGF–IL-8 interplay in tumor vascularization.

We hypothesized that alterations in VEGF and IL-8 secretion may partially relate to distinct biological distributions and functions of these angiogenic molecules, and their distribution in vitro and in vivo were next analyzed to address this possibility. A mathematical model of diffusion (Fig. 4*A*) suggested IL-8 would be present in higher concentrations than VEGF as one examined increasing distances from a tumor secreting these factors at the rates measured in 3D culture. These differences result from a combination of altered diffusion coefficients relating to their distinct molecular mass [VEGF, ≈45 kDa (25); IL-8, ≈8 kDa (26)], elimination rates, and secretion rates. Both VEGF165 and IL-8 contain heparin-binding domains (27, 28), suggesting that differential retention in the ECM likely does not control their diffusion. Specifically, IL-8 diffused more readily and was distributed over greater distances than VEGF; for example, at a distance of 100 μm from the tumor [corresponding to the critical distance for diffusion of nutrients from blood vessels (29)] the IL-8 concentration was 8 ng/mL, whereas VEGF was present at only 4 ng/mL (Fig. 4*A*). An experimental assay using focal injection of similar amounts of VEGF and IL-8 into Matrigel verified that differences in VEGF and IL-8 diffusion contribute to distinct spatial distributions of these factors in the tissue surrounding a tumor (Fig. 4*B*). Differential secretion and elimination of VEGF and IL-8 were not taken into account in this assay, resulting in quantitative differences

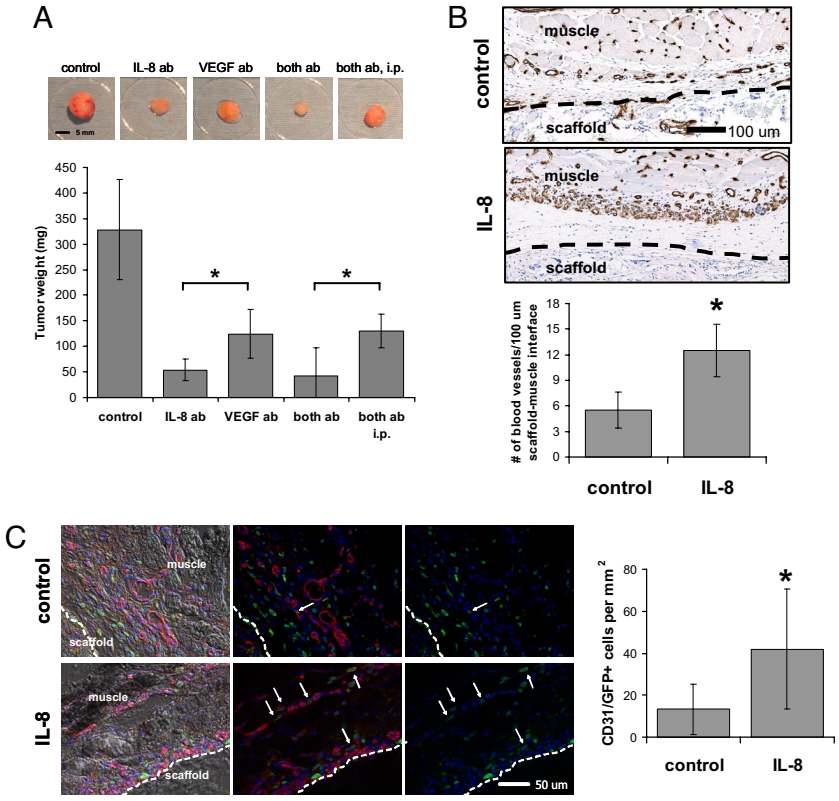

Fig. 5. Systemic and local effects of IL-8 on tumor vascularization and progression in vivo. (*A*) Antiangiogenic therapy using delivery of antibodies blocking IL-8 and VEGF either individually (IL-8 ab, VEGF ab) or simultaneously (both ab, both ab i.p.) inhibited tumor growth compared with the no-antibody control condition. Localized delivery of neutralizing IL-8 antibody (IL-8 ab) inhibited tumor progression more significantly compared with delivery of VEGF antibody (VEGF ab) ($P < 0.05$) and localized delivery of a regimen that consisted of both neutralizing IL-8 and neutralizing VEGF antibody (both ab) inhibited tumor formation more extensively relative to the same therapy systemically applied via i.p. injection (both ab i.p.) ($P < 0.05$). (*B*) Localized and sustained delivery of IL-8 from polymeric scaffolds as a mimic of IL-8 secretion from tumors (IL-8) resulted in increased blood vessel formation at the muscle–scaffold interface relative to implantation of blank control scaffolds (control) as determined by image analysis of histological cross-sections stained for the endothelial cell marker CD31 ($P < 0.05$). Inside the scaffold, blood vessel density was similar in both the control and IL-8 condition (data not shown). Dashed lines indicate the muscle–scaffold boundary. (*C*) Localized IL-8 release increased recruitment of bone marrow-derived cells (green) to the vasculature (red). IL-8 delivery from polymer scaffolds (IL-8) in mice transplanted with EGFP bone marrow led to more cells that costained for CD31 and EGFP, compared with mice transplanted with blank control scaffolds (control) ($P < 0.05$) as analyzed by coimmunofluorescence of cryosections (see Fig. S9 for confirmation of colocalization of staining). Arrows and dashed lines indicate double-labeled cells and the muscle–scaffold boundary, respectively.

between the computed and experimental diffusion assays. Analysis of VEGF, IL-8, and bFGF concentrations in tissues both immediately adjacent to tumors grown within RGD-alginate in SCID mice and in the systemic circulation of these mice further confirmed these findings. The IL-8 concentration in the local tumor environment was 3-fold higher than the VEGF and bFGF concentrations, and the serum IL-8 concentration was even more enhanced relative to VEGF (10-fold) and bFGF (8-fold) (Fig. S8). Calculation of the relative systemic factor concentrations suggested that IL-8 plays a more dominant role than the other factors in systemic signaling for tumor angiogenesis (Fig. 4*C*).

The relevance of enhanced local concentrations of IL-8 on tumor pathology and recruitment of vasculature in conjunction with VEGF was next evaluated. VEGF and IL-8 regulate tumor angiogenesis by different receptor signaling mechanisms, and simultaneous application of neutralizing antibodies may have an additive effect on the inhibition of cancer progression (23). Typically, antiangiogenic drugs are injected at extremely high concentrations, but this approach results in negative side effects at nontarget sites and may complicate investigations into the effect of enhanced local concentrations of proangiogenic molecules on tumor growth. Spatiotemporally controlled delivery of low concentrations of bioactive molecules from alginate-based delivery systems may overcome these limitations and may dramatically improve their therapeutic efficacy (30). Local delivery of relatively low amounts of neutralizing IL-8 and VEGF antibodies [i.e., 12.5% (IL-8 antibody) and 25% (VEGF antibody) of the dose applied in a recent study by Mizukami *et al.* (23) by i.p. injection] to tumors grown in vivo revealed that inhibition of VEGF decreased tumor growth, as expected, but blockade of IL-8 signaling inhibited tumor growth more significantly under these conditions. A combined delivery of both VEGF and IL-8 antibodies was equally efficacious in reducing tumor growth, and this localized delivery of the blocking antibodies inhibited tumor growth more efficiently relative to i.p. injection (Fig. 5*A*). These results indicate that normalization of systemic IL-8 levels may be therapeutically relevant; however, localized interference at the tumor source may be necessary to obtain optimal antiangiogenic effects.

IL-8 controls tumor vascularization by stimulating angiogenesis (21); however, it is not well understood to what extent enhanced levels of IL-8 regulate the homing of bone marrow-derived progenitor cells into the tumor vasculature. Exogenous IL-8 was provided in a biologically inspired manner by using a polymeric delivery vehicle as a mimic of IL-8 secretion from the tumor to determine specifically the role of elevated IL-8 signaling on angiogenesis in the absence of other potentially confounding variables (e.g., other factors secreted by tumor cells). Subcutaneous delivery of IL-8 from porous PLG scaffolds in C57BL/6J mice resulted in an enhanced blood vessel density at the scaffold–muscle interface (Fig. 5*B*), confirming a direct role of IL-8 in promoting vascularization in a localized manner. IL-8-releasing polymers were next implanted into EGFP bone marrow-transplanted mice to determine whether IL-8, with its significant long-range and systemic signal-

ing, enhances recruitment of bone marrow-derived cells mediating neovascularization. Coimmunostaining of tissue sections for CD31 and EGFP revealed that localized and sustained IL-8 delivery significantly increased the recruitment of bone marrow-derived cells to the vasculature at the scaffold–muscle interface relative to implantation of blank control scaffolds (Fig. 5*C*). These results suggest that up-regulated localized release of IL-8 may promote tumor growth and vascularization by promoting both angiogenic and vasculogenic processes.

In summary, 2D and 3D adhesion substrates were designed from alginate based biopolymers, and utilization of these synthetic ECMs revealed that 3D microenvironmental cues, in general, and 3D integrin engagement, in particular, are critical regulators of IL-8 secretion. Differential up-regulation of IL-8 may modulate tumor vascularization by affecting the molecular interplay with VEGF, and this alteration may be critical to the spatial control of tumor vascularization. Although this study was specifically designed to elucidate the role of 3D cell–ECM interactions, the alginate-based culture system described here may be broadly applicable to other questions in cancer research. They may, for example, be used to develop pathologically more relevant tumor models by integrating multiple cell types or to study specific signaling pathways by locally providing various combinations or sequences of bioactive molecules (31, 32). Because the mechanical rigidity of alginate-based adhesion substrates may be readily modulated, these synthetic ECMs may also be valuable in evaluating the role of altered mechanical stiffness of the tumor stroma in cancer progression. Furthermore, alginate-based artificial ECMs may be readily varied with regard to their bulk density and patterns of RGD peptide presentation while maintaining constant physicochemical properties, allowing for investigations of tumor vascularization and progression as a function of these parameters (33). Insights gained by these studies may improve our understanding of cancer and ultimately contribute to the development of more efficient anticancer therapies.

Materials and Methods

Two-Dimensional and 3D Adhesion Substrates. OSCC-3 (a gift from Peter Polverini; University of Michigan), U87 (American Type Culture Collection), and MDA-MB231 (American Type Culture Collection) were routinely cultured in DMEM/10% FBS. RGD peptide modification was carried out by covalently coupling GGGGRGDSP (Commonwealth Biotechnology) to sodium alginate (Pronova Biopolymers) by using standard carbodiimide chemistry as described in ref. 9; nonadhesive GGGGRGESP served as controls. The molar ratio of oligopeptides to sugar residues for RGD-alginate substrates was 0.0015:1. Calculations of RGD peptide density of tumor-associated ECM were based on the content of collagen type IV and laminin in Matrigel, a solubilized basement membrane preparation extracted from Engelbreth–Holm–Swarm mouse sarcoma. For 2D substrates, 2% alginate solutions were mixed with calcium sulfate (Sigma), cast between glass plates, and used for punching out topographically flat hydrogel disks. Excess calcium was leached out by daily medium changes for 4 days before seeding. To prepare 3D adhesion substrates, cells were suspended in 2% alginate solutions. By using a custom-designed encapsulation unit, the alginate–cell suspension was extruded into an isotonic $CaCl_2$ cross-linking solution. The generated beads were washed with PBS to remove excess Ca^{2+} and dynamically cultured in spinner flasks (Bellco Biotechnologies). For 3D alginate–bead studies, Cytodex-3 microcarriers beads (GE Healthcare Life Sciences) were coated with OSCC-3 and were subsequently encapsulated in alginate to yield a cell density per mL of alginate similar to all other conditions. Two-dimensional and 3D cell cultures were characterized as described in *SI Materials and Methods*.

Analysis of Growth Factor Diffusion. The mathematical diffusion model describes the spatial distribution profiles of VEGF and IL-8 in the tissue surrounding OSCC-3 tumors as a result of diffusion, elimination, and secretion (*SI Materials and Methods*). Fluorescence labeling of VEGF and IL-8 was performed with a Alexa Fluor 555 Microscale Protein Labeling Kit (Molecular Probes), and the diffusion assay was performed as described in *SI Materials and Methods*.

Analysis of Tumor Growth in Vivo. Biodegradable alginate implants were prepared from 5Mrad-irradiated RGD-alginate as described in ref. 34, and experimental animal procedures were performed in accordance with Harvard University animal care guidelines as outlined in *SI Materials and Methods*.

Analysis of Local and Systemic Effects of Up-Regulated IL-8. Porous scaffolds were fabricated from PLG (85:15, intrinsic viscosity 0.8 dL/g; Alkermes) to release 2 μg of recombinant human IL-8 (R&D) over a sustained period as described in ref. 35. Scaffolds were implanted into s.c. pockets in the back of C57BL/6J (Jackson Laboratories) mice transplanted with $EGFP^+$ bone marrow (*SI Materials and Methods*). Scaffolds were explanted 2 weeks after implantation, fixed, embedded in paraffin or OCT, and analyzed histologically (*SI Materials and Methods*).

ACKNOWLEDGMENTS. We thank Brian Tilton (Harvard University) for assistance with flow cytometry and Ross La Rosa and Paul Carman (Zeiss) for imaging support. This work was supported by National Institutes of Health Grant R01 HL069957 and by Portuguese Foundation for Science and Technology Fellowship SFRH/BD/13354/2003 (to M.B.E.).

1. Debnath J, Brugge JS (2005) Modelling glandular epithelial cancers in 3-dimensional cultures. *Nat Rev Cancer* 5:675–688.
2. Wang F, *et al.* (1998) Reciprocal interactions between β1-integrin and epidermal growth factor receptor in 3-dimensional basement membrane breast cultures: A different perspective in epithelial biology. *Proc Natl Acad Sci USA* 95:14821–14826.
3. Fischbach C, *et al.* (2007) Engineering tumors with 3D scaffolds. *Nat Methods* 4:855–860.
4. Paszek MJ, *et al.* (2005) Tensional homeostasis and the malignant phenotype. *Cancer Cell* 8:241–254.
5. Hanahan D, Weinberg RA (2000) The hallmarks of cancer. *Cell* 100:57–70.
6. De S, *et al.* (2005) VEGF–integrin interplay controls tumor growth and vascularization. *Proc Natl Acad Sci USA* 102:7589–7594.
7. Lowrie AG, Salter DM, Ross JA (2004) Latent effects of fibronectin, $\alpha5\beta1$ integrin, $\alpha v\beta5$ integrin, and the cytoskeleton regulate pancreatic carcinoma cell IL-8 secretion. *Br J Cancer* 91:1327–1334.
8. Cukierman E, Pankov R, Stevens DR, Yamada KM (2001) Taking cell matrix adhesions to the third dimension. *Science* 294:1708–1712.
9. Rowley JA, Madlambayan G, Mooney DJ (1999) Alginate hydrogels as synthetic extracellular matrix materials. *Biomaterials* 20:45–53.
10. Lingen MW (1999) Angiogenesis in the development of head and neck cancer and its inhibition by chemopreventive agents. *Crit Rev Oral Biol Med* 10:153–164.
11. Fischbach C, Mooney D (2006) Polymeric systems for bioinspired delivery of angiogenic molecules. *Adv Polym Sci* 203:191–221.
12. Ruoslahti E, Pierschbacher MD (1987) New perspectives in cell adhesion: RGD and integrins. *Science* 238:491–497.
13. Kong HJ, Boontheekul T, Mooney DJ (2006) Quantifying the relation between adhesion ligand–receptor bond formation and cell phenotype. *Proc Natl Acad Sci USA* 103:18534–18539.
14. Harris AL (2002) Hypoxia: A key regulatory factor in tumour growth. *Nat Rev Cancer* 2:38–47.
15. Xu L, *et al.* (1999) Hypoxia-induced elevation in interleukin-8 expression by human ovarian carcinoma cells. *Cancer Res* 59:5822–5829.
16. Weaver VM, *et al.* (1997) Reversion of the malignant phenotype of human breast cells in three-dimensional culture and in vivo by integrin-blocking antibodies. *J Cell Biol* 137:231–245.
17. Chung J, *et al.* (2004) Hypoxia-induced vascular endothelial growth factor transcription and protection from apoptosis are dependent on $\alpha6\beta1$ integrin in breast carcinoma cells. *Cancer Res* 64:4711–4716.
18. Ghosh S, *et al.* (2005) Three-dimensional culture of melanoma cells profoundly affects gene expression profile: A high density oligonucleotide array study. *J Cell Physiol* 204:522–531.
19. De Larco JE, *et al.* (2001) A potential role for interleukin-8 in the metastatic phenotype of breast carcinoma cells. *Am J Pathol* 158:639–646.
20. Nemeth ZH, *et al.* (2004) Disruption of the actin cytoskeleton results in nuclear factor-κB activation and inflammatory mediator production in cultured human intestinal epithelial cells. *J Cell Physiol* 200:71–81.
21. Xie K (2001) Interleukin-8 and human cancer biology. *Cytokine Growth Factor Rev* 12:375–391.
22. Casanovas O, Hicklin DJ, Bergers G, Hanahan D (2005) Drug resistance by evasion of antiangiogenic targeting of VEGF signaling in late-stage pancreatic islet tumors. *Cancer Cell* 8:299–309.
23. Mizukami Y, *et al.* (2005) Induction of interleukin-8 preserves the angiogenic response in HIF-1α-deficient colon cancer cells. *Nat Med* 11:992–997.
24. Esposito I, *et al.* (2004) Inflammatory cells contribute to the generation of an angiogenic phenotype in pancreatic ductal adenocarcinoma. *J Clin Pathol* 57:630–636.
25. Ferrara N, Henzel WJ (1989) Pituitary follicular cells secrete a novel heparin-binding growth factor specific for vascular endothelial cells. *Biochem Biophys Res Commun* 161:851–858.
26. Gaertner HF, Offord RE (1996) Site-specific attachment of functionalized poly(ethylene glycol) to the amino terminus of proteins. *Bioconjug Chem* 7:38–44.
27. Goerges AL, Nugent MA (2003) Regulation of vascular endothelial growth factor binding and activity by extracellular pH. *J Biol Chem* 278:19518–19525.
28. Kuschert GS, *et al.* (1998) Identification of a glycosaminoglycan binding surface on human interleukin-8. *Biochemistry* 37:11193–11201.
29. Kerbel R, Folkman J (2002) Clinical translation of angiogenesis inhibitors. *Nat Rev Cancer* 2:727–739.
30. Fischbach C, Mooney DJ (2007) Polymers for pro- and antiangiogenic therapy. *Biomaterials* 28:2069–2076.
31. Alsberg E, *et al.* (2002) Engineering growing tissues. *Proc Natl Acad Sci USA* 99:12025–12030.
32. Simmons CA, *et al.* (2004) Dual growth factor delivery and controlled scaffold degradation enhance in vivo bone formation by transplanted bone marrow stromal cells. *Bone* 35:562–569.
33. Comisar WA, Kazmers NH, Mooney DJ, Linderman JJ (2007) Engineering RGD nanopatterned hydrogels to control preosteoblast behavior: A combined computational and experimental approach. *Biomaterials* 28:4409–4417.
34. Alsberg E, *et al.* (2003) Regulating bone formation via controlled scaffold degradation. *J Dent Res* 82:903–908.
35. Richardson TP, Peters MC, Ennett AB, Mooney DJ (2001) Polymeric system for dual growth factor delivery. *Nat Biotechnol* 19:1029–1034.